Slowness vectors in viscoelastic anisotropic media. Part 2: Numerical examples

Vlastislav Červený [1), Ivan Pšenčík [2)

1) Department of Geophysics, Faculty of Mathematics and Physics, Charles University, Ke Karlovu 3, 121 16 Praha 2, Czech Republic. E-mail vcerveny@seis.karlov.mff.cuni.cz
2) Geophysical Institute, Acad. Sci. of Czech Republic, Boční II, 141 31 Praha 4, Czech Republic. E-mail ip@ig.cas.cz

Summary

The expressions based on the so-called mixed specification of the slowness vector of plane waves propagating in viscoelastic anisotropic media, derived by Červený and Pšenčík (2004), are used to illustrate behaviour of various characteristics of these plane waves. Studied characteristics are phase velocities, amplitude decay along the propagation direction, attenuation, attenuation angle and polarization vectors. Simple analytic expressions are used to describe behaviour of SH waves propagating in a plane of symmetry of a viscoelastic anisotropic medium. Characteristics of qP plane wave and qS plane waves are determined by solving a complex-valued algebraic equation of the sixth degree. Combined effects of attenuation and anisotropy predicted in Červený and Pšenčík (2004) are illustrated on two models of viscoelastic anisotropic media. The explanation of the so-called forbidden directions known from the directional specification of the slowness vector is given. Non-physical results related to forbidden directions do not arise in the mixed specification.

Keywords
Viscoelastic anisotropic media, inhomogeneous and homogeneous plane waves, mixed specification, inhomogeneity parameter, phase velocity, attenuation, attenuation angle, polarization.

1 Introduction

Many parts of the Earth's interior display seismic anisotropy and attenuation. Considerable attention has been devoted to wave propagation in elastic anisotropic or dissipative isotropic media. Study of wave propagation in anelastic anisotropic media, however, still deserves attention. Such a study is necessary for correct modelling of seismic wave propagation in anelastic anisotropic media as well as for understanding the phenomena related

Seismic Waves in Complex 3-D Structures, Report 14 (Department of Geophysics, Charles University, Prague 2004), pp.149-179

to such propagation. We concentrate on viscoelastic anisotropic media specified by a tensor of complex-valued frequency-dependent density-normalized viscoelastic moduli a_{ijkl} whose real parts are positively definite and imaginary parts are zero or negatively definite with respect to pairs of indices i, j and k, l. We study several characteristics describing propagation of a harmonic plane wave with an arbitrarily chosen but fixed positive frequency through such a medium.

For the study, we use the formulae derived by Červený (2004) and Červený and Pšenčík (2004) for the so-called *mixed specification* of the complex-valued slowness vector

$$\mathbf{p} = \sigma\mathbf{n} + \mathrm{i}D\mathbf{m}. \tag{1}$$

Here, $\mathbf{n}$ and $\mathbf{m}$ are two mutually perpendicular, real-valued unit vectors, assumed to be known. The vector $\mathbf{n}$ represents a normal to the plane of constant phase, i.e., to the wavefront. It may point in the direction of propagation (direction of the real part of the slowness vector $\mathbf{p}$) if real part of σ is positive or against it if real part of σ is negative. The vector $\mathbf{m}$ is tangent to the wavefront. The vectors $\mathbf{n}$ and $\mathbf{m}$ define the *propagation-attenuation plane* $\Sigma^{\|}$, in which the considered complex-valued slowness vector $\mathbf{p}$ is situated. The real-valued quantity D, $(-\infty < D < \infty)$, called the *inhomogeneity parameter*, is also assumed to be known. Its absolute value $|D|$ characterizes inhomogeneity (deviation from homogeneity) of the wave, and it is, therefore, called the *strength of inhomogeneity*. The complex-valued quantity σ, which represents the projection of the slowness vector $\mathbf{p}$ to vector $\mathbf{n}$, is a sought quantity. It can be determined from the condition following from the requirement that the plane wave with the slowness vector (1) satisfies the elastodynamic equation, see Červený (2004) and Červený and Pšenčík (2004). For unrestricted anisotropy and viscoelasticity, the condition for the determination of σ can be expressed in terms of a sixth-degree algebraic equation. Thus the task to find the slowness vector for given vectors $\mathbf{n}$, $\mathbf{m}$ and an inhomogeneity parameter D in a general viscoelastic anisotropic medium reduces to solving this algebraic equation. An alternative way is to seek σ as the eigenvalues of a 6×6 complex-valued matrix (Červený and Pšenčík, 2004). Here, we use the former approach based on the solution of the algebraic equation. This is incomparably simpler than with approaches commonly used in isotropic viscoelastic media, see detailed discussion in Červený and Pšenčík (2004). The mixed specification is thus a natural and convenient tool for study of details of plane wave propagation in general viscoelastic anisotropic media.

We study behaviour of several characteristics of homogeneous and inhomogeneous plane waves in viscoelastic media, specifically phase velocities, imaginary parts of the parameter σ (which describe exponential decay of plane-wave amplitudes in the direction of propagation), attenuation, attenuation angle and polarization. We have to keep in mind that we study all the mentioned characteristics with respect to the direction of propagation specified by the vector $\mathbf{n}$ and not with respect to the direction of energy flux. In the latter case, behaviour of the above-listed characteristics would look differently. First we concentrate on SH plane waves propagating in a plane of symmetry of a viscoelastic anisotropic medium. Červený and Pšenčík (2004) derived simple analytic expressions for this case, which are used for the evaluation of characteristics of SH plane waves. Next we study all three waves propagating in anisotropic viscoelastic media. In this case, numerical solution of a sixth-degree algebraic equation is sought. Analysis of the obtained results reveals series of phenomena unfamiliar from studies of plane-wave propagation in elastic anisotropic or viscoelastic isotropic media. The phenomena are discussed in a detail in the paper.

In Sec.2, basic equations for the mixed specification of a slowness vector given in Červený and Pšenčík (2004) are summarized. These equations are used in the computations, whose results are presented in the following sections. In Sec.3, analysis of results obtained for SH waves from simple analytic formulae is made. The results for SH plane waves propagating in a symmetry plane of a viscoelastic anisotropic medium are compared with results of the same formulae for a viscoelastic isotropic medium. In Sec.4, analogous results for all three waves propagating in viscoelastic anisotropic media are analysed. Sec.5 contains detailed explanation of the phenomenon of forbidden directions, and Sec.6 some concluding remarks.

2 Basic equations

As shown by Červený and Pšenčík (2004), the specification (1) leads to a system of linear equations

$$a_{ijkl}(\sigma n_j + \mathrm{i}Dm_j)(\sigma n_l + \mathrm{i}Dm_l)U_k = U_i, \quad i = 1, 2, 3 \tag{2}$$

for the polarization vector $\mathbf{U}$ and to the algebraic equation of the sixth degree

$$\det[a_{ijkl}(\sigma n_j + \mathrm{i}Dm_j)(\sigma n_l + \mathrm{i}Dm_l) - \delta_{ik}] = 0 \tag{3}$$

for the quantity σ. In (2) and (3), a_{ijkl} are complex-valued density-normalized viscoelastic moduli specified for a fixed frequency. Eq.(3) is a polynomial equation with coefficients, which are generally complex-valued. For the coefficients, see Fedorov (1968) (note misprints in the coefficients with powers 5 and 2). Eq.(3) has six roots corresponding to qS1, qS2 and qP plane waves propagating in the directions of $\pm\mathbf{n}$. Various methods can be used to solve Eq.(3), see Červený (2004). Here we either evaluate an analytic solution of Eq.(3) derived by Červený and Pšenčík (2004) for the propagation of SH plane waves in a plane of symmetry of a viscoelastic anisotropic medium, or solve Eq.(3) numerically, using the Laguerre's method, see Press et al.(1986).

We consider inhomogeneous plane waves with vectors $\mathbf{n}$ and $\mathbf{m}$ confined to the plane (x_1, x_3), i.e., the plane (x_1, x_3) is the propagation-attenuation plane. This means that the components of the vectors $\mathbf{n}$ and $\mathbf{m}$ can be expressed as

$$n_1 = \sin i, \quad n_2 = 0, \quad n_3 = \cos i, \qquad m_1 = \cos i, \quad m_2 = 0, \quad m_3 = -\sin i. \tag{4}$$

Here i is the propagation angle.

The slowness vector $\mathbf{p}$ can be written alternatively as

$$\mathbf{p} = \mathbf{P} + \mathrm{i}\mathbf{A}, \tag{5}$$

where the real-valued vector $\mathbf{P}$ is the *propagation vector*, $\mathbf{P} = |\mathbf{P}|\mathbf{N}$, the real-valued vector $\mathbf{A}$ is the *attenuation vector*, $\mathbf{A} = |\mathbf{A}|\mathbf{M}$, $\mathbf{N}$ and $\mathbf{M}$ being real-valued unit vectors. The vectors $\mathbf{N}$ and $\mathbf{M}$ make an angle γ called the *attenuation angle*, $\cos\gamma = \mathbf{N} \cdot \mathbf{M}$.

By comparing Eqs.(5) and (1), we can see that the direction of the propagation vector $\mathbf{P} = \mathrm{Re}\sigma\ \mathbf{n}$ is parallel to the vector $\mathbf{n}$ and points along or against it depending on the sign of $\mathrm{Re}\sigma$. Therefore, $\mathbf{N} = \pm\mathbf{n}$. The attenuation vector $\mathbf{A} = \mathrm{Im}\sigma\ \mathbf{n} + D\mathbf{m}$ has, in general, projections into $\mathbf{n}$ and $\mathbf{m}$. For $D = 0$ (homogeneous wave), the attenuation vector is parallel to $\mathbf{n}$ and points along or against it depending on the sign of $\mathrm{Im}\sigma$. For $\mathrm{Im}\sigma = 0$ and $D \neq 0$ (inhomogeneous waves in isotropic elastic media), the attenuation vector is parallel to $\mathbf{m}$.

From Eq.(5), we get simply the *directional specification* of the slowness vector discussed by Červený and Pšenčík (2004),

$$\mathbf{p} = \mathcal{C}^{-1}(\mathbf{N} + \mathrm{i}\delta\mathbf{M}). \tag{6}$$

In the directional specification, the vectors $\mathbf{N}$ and $\mathbf{M}$ are assumed to be known; thus the attenuation angle γ is also known. The phase velocity $\mathcal{C}$ and the attenuation-propagation ratio δ are sought quantities. Eq.(6) represents the most common specification of the complex-valued slowness vector in seismological literature.

For a value of σ determined by solving Eq.(3), the relevant propagation vector $\mathbf{P}$, attenuation vector $\mathbf{A}$, vectors $\mathbf{N}$ and $\mathbf{M}$, phase velocity $\mathcal{C}$, attenuation-propagation ratio δ and attenuation angle γ, related to the inhomogeneous plane wave under consideration can be determined from the formulae (Červený and Pšenčík, 2004):

$$\begin{array}{ll}
P_1 = n_1(\mathrm{Re}\sigma)\ , & A_1 = n_1(\mathrm{Im}\sigma) + n_3 D\ , \\
P_3 = n_3(\mathrm{Re}\sigma)\ , & A_3 = n_3(\mathrm{Im}\sigma) - n_1 D\ , \\
|\mathbf{P}| = |\mathrm{Re}\sigma|\ , & |\mathbf{A}| = [(\mathrm{Im}\sigma)^2 + D^2]^{1/2}\ , \\
N_1 = \epsilon\ n_1\ , & M_1 = [n_1(\mathrm{Im}\sigma) + n_3 D]/[(\mathrm{Im}\sigma)^2 + D^2]^{1/2}\ , \\
N_3 = \epsilon\ n_3\ , & M_3 = [n_3(\mathrm{Im}\sigma) - n_1 D]/[(\mathrm{Im}\sigma)^2 + D^2]^{1/2}\ , \\
\mathcal{C} = 1/|\mathrm{Re}\sigma|\ , & \delta = [(\mathrm{Im}\sigma)^2 + D^2]^{1/2}/|\mathrm{Re}\sigma|\ , \\
\cos\gamma = \epsilon\,\mathrm{Im}\sigma/[(\mathrm{Im}\sigma)^2 + D^2]^{1/2}\ . &
\end{array} \tag{7}$$

Here, ϵ is given by

$$\epsilon = \mathrm{Re}\sigma/|\mathrm{Re}\sigma| = \pm 1\ . \tag{8}$$

In the propagation-attenuation plane $\Sigma^{\parallel}$, which is identical with the plane (x_1, x_3), $P_2 = A_2 = N_2 = M_2 = 0$.

In the following, we study properties of inhomogeneous plane waves in propagation-attenuation plane $\Sigma^{\parallel}$. In this plane, the waves are specified by two parameters: the propagation angle i and the inhomogeneity parameter D. Two types of pictures are presented: (i) For i fixed, considering varying inhomogeneity parameter D. (ii) For D fixed, considering variation of the propagation angle i (polar graphs). In the pictures, the phase velocity $\mathcal{C}$ is measured in km/s, the quantity σ, the attenuation $|\mathbf{A}|$ and inhomogeneity parameter D in $(\mathrm{km/s})^{-1}$, and the propagation angle i and the attenuation angle γ in degrees. The frequency is kept constant in all studies.

3 SH plane waves in a symmetry plane

In this section, we discuss the properties of SH inhomogeneous plane waves, propagating in the plane of symmetry Σ^S of a monoclinic anisotropic viscoelastic medium. We assume that Σ^S is identical with the propagation-attenuation plane $\Sigma^{\parallel}$, and both planes coincide with the plane (x_1, x_3). As shown in Eq.(57) of Červený and Pšenčík (2004), Eq.(3) has two simple analytic solutions in this case:

$$\sigma_{1,2} = -\mathrm{i}D\Lambda\Gamma_{22}^{-1} \pm [\Gamma_{22}^{-1} + D^2\Gamma_{22}^{-2}\Delta]^{1/2}, \tag{9}$$

where

$$\begin{aligned} \Gamma_{22} &= A_{66}n_1^2 + A_{44}n_3^2 + 2A_{46}n_1n_3, \\ \Lambda &= (A_{66} - A_{44})n_1n_3 + A_{46}(n_3^2 - n_1^2), \\ \Delta &= A_{44}A_{66} - A_{46}^2, \end{aligned} \tag{10}$$

and D is the inhomogeneity parameter. The quantities A_{44}, A_{46} and A_{66} are the density-normalized viscoelastic moduli in the Voigt notation. The two values of σ correspond to the two SH waves propagating in the directions of $\pm\mathbf{n}$.

The model of viscoelastic anisotropic medium used is close to that used by Carcione and Cavallini (1995) in the computations based on the directional specification of the slowness vector of an SH wave. The density-normalized viscoelastic moduli are:

$$A_{44} = 5 - \mathrm{i}\ , \qquad A_{66} = 11.25 - 1.125\mathrm{i}\ , \qquad A_{46} = 2.5\ . \tag{11}$$

All quantities in (11) have dimensions $(\mathrm{km/s})^2$. Both anisotropy and dissipation considered in (11) are rather strong. We therefore present also additional results for models closer to isotropy and perfect elasticity.

3.1 SH plane waves in isotropic viscoelastic media: variations with D

To study the effects of anisotropy on inhomogeneous plane waves, it is useful to start with some reference results for isotropic viscoelastic media. The properties of plane waves in isotropic viscoelastic media have been extensively studied in seismological literature. For a list of selected references see Červený and Pšenčík (2004). In most of the studies, the attenuation angle γ was used as a basic parameter specifying slowness vectors of inhomogeneous plane waves. Here, as in the whole text, we consider the mixed specification of the slowness vector, and use the inhomogeneity parameter D as a basic parameter.

For isotropic viscoelastic media, the equation for $\sigma_{1,2}$ follows from Eqs.(9) and (10), if we take into account that $A_{44} = A_{66}$ and $A_{46} = 0$. We then obtain a very simple expression

$$\sigma_{1,2} = \pm[1/\beta^2 + D^2]^{1/2}\ . \tag{12}$$

Here β is the complex-valued S-wave velocity, $\beta^2 = A_{44}$, which is independent of the propagation angle i. Thus, the values $\sigma_{1,2}$ are also independent of the propagation angle. Equation (12) is valid generally, for homogeneous and inhomogeneous plane waves, propagating in viscoelastic and perfectly elastic media. It even holds for P waves, if we substitute the S-wave velocity β by the P-wave velocity α. Inserting (12) into (7), we can evaluate various characteristics of S waves propagating in isotropic viscoelastic media.

Let us illustrate behaviour of some of the quantities listed in (7) in viscoelastic isotropic models close to the anisotropic viscoelastic model (11). The models are obtained by varying imaginary part of the square of the S-wave velocity:

$$\beta^2 = 5 - \mathrm{i}\nu \ . \qquad (13)$$

In (13), we consider the following values of ν: ν=1, 0.5, 0.25 and 0. If we express β^2 in terms of the real-valued S-wave velocity V_S and the quality factor Q_S so that $\beta^2 = V_S^2(1 - \mathrm{i}/Q_S)$, we obtain $V_S^2 = 5$ and $Q_S = 5, 10, 20$ and ∞, respectively.

In the following, we study behaviour of selected characteristics of SH plane waves as functions of the inhomogeneity parameter D. The results are independent of the propagation angle i. Fig.1 displays the variations of $\mathcal{C}, \mathrm{Im}\sigma, |\mathbf{A}|$ and γ with $D, D \in (-0.2, 0.2)$. Each frame of Fig.1 shows black, red, green and blue curves corresponding to (13) with ν=1, 0.5, 0.25 and 0, respectively. Let us list the most important observations:

1) All curves are **symmetric** with respect to $D = 0$, which correspods to a homogeneous plane wave.

2) The **phase velocities** $\mathcal{C}$ depend only slightly on the value of Q_S, for D fixed. For example, for $D = 0$, they increase from 2.236 km/s for the perfectly elastic case ($Q_S = \infty$, blue) to 2.269 km/s for $Q_S = 5$ (black). They, however, change more strongly with increasing inhomogeneity strength $|D|$. The maximum phase velocity is always obtained for the homogeneous plane wave ($D = 0$). It follows from (7) and (12) that $\mathcal{C} \to 0$ for $|D| \to \infty$.

3) The **values of Im**σ, controlling the amplitude decay along the propagation vector $\mathbf{P}$, are zero for perfectly elastic isotropic medium (blue), and positive for an viscoelastic isotropic medium. This means that the exponential decay of amplitudes is always positive along the direction of propagation in isotropic viscoelastic media. The values of $\mathrm{Im}\sigma$ depend considerably on the dissipative properties of the medium; they increase considerably with decreasing value of the quality factor Q_S. $\mathrm{Im}\sigma$ is practically independent of D, at least for small D. Only for strongly dissipative media, $\mathrm{Im}\sigma$ slightly decreases with increasing $|D|$. Note that the zero value of $\mathrm{Im}\sigma$ for perfectly elastic isotropic medium does not mean that inhomogeneous plane waves do not propagate in perfectly elastic media. Zero $\mathrm{Im}\sigma$ only indicates that there is no exponential decay in the direction $\mathbf{n}$. As $\mathbf{p} = \sigma\mathbf{n} + \mathrm{i}D\mathbf{m}$, the exponential decay of an inhomogeneous plane wave propagating in an elastic isotropic medium is always in the direction $\mathbf{m}$. This means that homogeneous plane waves do not exist in perfectly elastic media.

4) The **attenuation** $|\mathbf{A}|$ has a hyperbolic form for varying D, with a minimum for $D = 0$ (homogeneous plane waves). With the exception of very small $|D|$, it increases approximately linearly with $|D|$, and depends only slightly on the quality factor Q_S. For perfectly elastic media, Eqs.(7) and (12) yield exactly $|\mathbf{A}| = |D|$.

5) The most interesting results are obtained for the **attenuation angle** γ. It is well known from classical studies that the attenuation angle in isotropic, perfectly elastic or viscoelastic media never exceeds 90^0. For perfectly elastic isotropic medium (blue curve), the attenuation angle γ equals always 90^0. Behaviour of γ in viscoelastic isotropic media with respect to D is very interesting for small D. For $D = 0$ (homogeneous plane waves), γ is zero. The value of γ, however, increases very fast with $|D|$ increasing, and for $|D| \to \infty$,

it approaches 90^0. The increase is faster and more concentrated to small $|D|$ for increasing values of the quality factor Q_S.

Let us emphasize that the value of σ varies very slowly with D for small values of $|D|$, see plots for $\mathcal{C} = 1/|\mathrm{Re}\sigma|$ and $\mathrm{Im}\sigma$. Thus, the expression (12) for σ can be simply used in the perturbation methods, particularly for weakly dissipative media. Eq.(12) can be also expanded to yield approximate linear or quadratic expressions for σ in terms of D. This is impossible if we use directional specification of the slowness vector in terms of the attenuation angle γ. Specifically for $|D|$ small and for weakly dissipative media, the attenuation angle γ is varying extremely fast. In fact, this is well known from the classical studies, in which the expressions for the slowness vector contain the product $Q_S \cos\gamma$, see, for example, Aki and Richards (1980, Eq. (5.96)). In the limiting case of perfectly elastic media, this product is indefinite (as $Q_S = \infty, \gamma = 90^0$). Thus for weakly dissipative media, which are the main object of our interest, $Q_S \cos\gamma$ is very unstable. All these difficulties are removed by considering the mixed specification of the slowness vector and using the inhomogeneity parameter D instead of γ.

3.2 SH plane waves in a symetry plane of anisotropic viscoelastic media: variations with D

In this section, we discuss numerical results describing properties of SH plane waves, propagating in the plane of symmetry Σ^S of a monoclinic anisotropic viscoelastic medium. Let us emphasize that propagation of SH plane waves in symmetry planes of transversely isotropic and monoclinic viscoelastic media has been studied by Krebes and Le (1994) and Carcione and Cavallini (1995), respectively. They used the directional specification of the slowness vector. As in Sec.3.1, we study here various characteristics of homogeneous and inhomogeneous plane waves as functions of the inhomogeneity parameter D, with the propagation angle i fixed.

As the reference viscoelastic anisotropic model, we consider model specified by the density-normalized complex-valued viscoelastic moduli A_{44}, A_{66} and A_{46}, given by (11). In Figs.2 and 3, results corresponding to the model (11) are denoted by black curves. The red and green curves correspond to the twice and four times smaller imaginary parts in (11), and the blue curve corresponds to the relevant perfectly elastic anisotropic medium. Specifically, the values of $\mathrm{Im}A_{44}$, $\mathrm{Im}A_{66}$, and $\mathrm{Im}A_{46}$ are successively: -1, -1.125, 0 (black), -0.5, -0.5625, 0 (red), -0.25, -0.28125, 0 (green), and 0, 0, 0 (blue). The propagation angle i equals 45^0 in Fig.2 and 135^0 in Fig.3. Let us first discuss Fig.2, corresponding to the propagation angle $i = 45^0$, and let us list the most important observations:

1) All curves plotted in Fig.2 are, in contrast to Fig.1, **non-symmetric** with respect to $D = 0$.

2) Behaviour of **phase velocities** in anisotropic viscoelastic media has some features similar to those in isotropic viscoelastic media. The phase velocities depend only slightly on the dissipative parameters of the media. For example, for homogeneous plane waves ($D = 0$), the phase velocities for the four models are successively: 3.27178, 3.26265, 3.26036, and 3.25960 km/s. For $|D| \to \infty$, the phase velocities decrease to zero. There

are, however, certain differences between behaviour of phase velocities in isotropic and anisotropic viscoelastic media: phase velocities $\mathcal{C}$ in viscoelastic anisotropic media do not attain their maximum value $\mathcal{C}^M$ for $D = 0$ (homogeneous plane wave) as in isotropic viscoelastic media, but for $D = D^M \neq 0$ (inhomogeneous plane wave). The shift of the maximum phase velocity from $D = 0$ to $D = D^M$ is small but observable, see Fig.2. Approximate analytic expressions for D^M and $\mathcal{C}^M$ are given in Eqs.(68)–(69) of Červený and Pšenčík (2004). If we take into account that the phase velocity of the homogeneous plane wave $\mathcal{C}_{hom}$ equals $1/a$, we obtain $\mathcal{C}^M - \mathcal{C}_{hom} \doteq b^2/4c\,a^2 > 0$. For a, b and c, see (67) of Červený and Pšenčík (2004). We can also see that for negative values of D the highest phase velocities are in the most attenuating model (black) while for positive values of D the highest phase velocities are in the perfectly elastic model (blue).

We give several quantitative results related to D^M and $\mathcal{C}^M - \mathcal{C}_{hom}$ for the models under consideration. For the black curve, $D^M = -0.0160$, $\mathcal{C}^M - \mathcal{C}_{hom} = 0.001995$ km/s, for the red curve $D^M = -0.0080$ and $\mathcal{C}^M - \mathcal{C}_{hom} = 0.000506$ km/s, and for the green curve $D^M = -0.0040$ and $\mathcal{C}^M - \mathcal{C}_{hom} = 0.000127$ km/s. It is not difficult to verify that the approximate relations (68) and (69) of Červený and Pšenčík (2004) give approximately the same results.

3) There is a great difference between behaviour of **Im**σ for viscoelastic isotropic and viscoelastic anisotropic media. For isotropic media, Imσ is always non-negative, and depends only very slightly on D, but strongly on dissipative parameters. For anisotropic viscoelastic media, however, it varies roughly linearly with D for small $|D|$. Dependence on dissipative parameters is much weaker. For small $|D|$, a simple approximate analytical relation (70) of Červený and Pšenčík (2004) holds for $D = D_0$, for which Im$\sigma = 0$. For the models used in Fig.2, and for the propagation angle $i = 45^0$, the factor $\Lambda\Gamma_{22}^{-1}$ in Eq.(9) is positive and Imσ thus decreases with increasing D. We obtain $D_0 = 0.0511$ for the black, $D_0 = 0.02580$ for the red, and $D_0 = 0.0131$ for the green curve. For perfectly elastic case (blue), $D_0 = 0$, as simply follows from inspection of Eq.(9). For $D < D_0$, Imσ is positive, and for $D > D_0$, it is negative.

The positive value of Imσ has a standard meaning: the amplitudes of inhomogeneous plane waves decay exponentially in the direction of the vector $\mathbf{N}$. The existence of negative Imσ (for $D > D_0$) means exponential **growth** of amplitudes in the direction of the propagation $\mathbf{N}$ for $D > D_0$. An analogous apparent paradox has been discovered in the studies of inhomogeneous SH plane waves, based on the directional specification (6) of the slowness vector (with fixed γ), see Krebes and Le (1994), Carcione and Cavallini (1995), Carcione (2001). Physical explanation consists in the fact that the inhomogeneous plane waves always decay exponentially in the direction of the energy flux, which generally differs from the direction of the wave propagation ($\mathbf{N}$) in viscoelastic anisotropic media. Here we do not discuss the energy flux of inhomogeneous plane waves, but specify quantitatively the values of inhomogeneity parameter D_0, which separates regions of amplitude growth and decay along the propagation vector.

4) Behaviour of the **attenuation** $|\mathbf{A}|$ for fixed i and D varying, is not very different for isotropic and anisotropic viscoelastic media; compare Figs.1 and 2. Similarly as in isotropic viscoelastic media, the curves have a hyperbolic form. With the exception of very small $|D|$, the curves increase approximately linearly with increasing $|D|$. There is, however, one small, but remarkable difference. In anisotropic viscoelastic media, the

minima A_{min} of the attenuation curves are not situated at $D = 0$ (homogeneous waves), but at $D = D_{att} \neq 0$ (inhomogeneous waves). This has been predicted in Eq.(71) of Červený and Pšenčík (2004). The shift is small, but it is clearly observable in Fig.2. Let us present numerical values, corresponding to the models under consideration. For the blue curve (perfect elasticity), $D_{att} = 0$ with $A_{min} = 0$, for the black curve, $D_{att} = 0.0041$ with $A_{min} = 0.0146$, for the red curve $D_{att} = 0.0021$ with $A_{min} = 0.0073$, and for the green curve, $D_{att} = 0.0010$ with $A_{min} = 0.0036$. This effect might be more expressive for other propagation angles i; see, for example, Fig.3. Let us note that for perfectly elastic media, Eqs.(7) and (9) yield $|\mathbf{A}| = |D|[1 + \Lambda^2\Gamma_{22}^{-2}]^{1/2}$.

5) Certain properties of the **attenuation angle** γ of SH waves in anisotropic viscoelastic media remain similar to those in isotropic viscoelastic media. For $D = 0$, the attenuation angle γ is zero, and increases fast with $|D|$ increasing. For $|D| \to \infty$, the attenuation angle γ reaches its boundary values γ^*. The increase of γ with increasing $|D|$ is particularly fast for small $|D|$, in weakly dissipative media. In certain other aspects, the properties of the attenuation angle γ are very different in isotropic and anisotropic viscoelastic media. Let us discuss briefly the most important differences in the behaviour of γ by comparing Figs.1 and 2.

The values of γ are not symmetrical with respect to $D = 0$, $\gamma(D) \neq \gamma(-D)$. Consequently, the boundary values γ^* (for infinite $|D|$) are different for $D \to \infty$ and $D \to -\infty$. The values of boundary attenuation angle γ^* are different from 90^0. As a rule, γ^* exceeds 90^0 for one sign of D, and is less than 90^0 for the other sign of D.

Let us present values of boundary attenuation angles γ^* corresponding to the four models used in Fig.2. For $D > 0$, the values of γ^* are: 108.60^0, 107.55^0, 106.98^0 and 106.39^0 (for the elastic case). For $D < 0$, they are: 76.13^0, $74.85^0, 74.22^0$ and 73.61^0 (for the elastic case). As we can see, the boundary attenuation angles γ^* for viscoelastic anisotropic media are very close to the attenuation angles for relevant perfectly elastic anisotropic media. In our case, the difference for the model (11) does not exceed 2.6^0, even though the model (11) is strongly dissipative and strongly anisotropic. The value of γ for perfectly elastic anisotropic media is discontinuous at $D = 0$. It has different constant values for $D > 0$ and for $D < 0$, which are symmetric with respect to 90^0 as follows from (7) and (9). The values are the same and equal to 90^0 only when $\Lambda = 0$, i.e. when $(A_{66} - A_{44}) \sin 2i + 2A_{46} \cos 2i = 0$. For all other propagation angles i, the attenuation angle γ is different from 90^0 although it may be close to it (for small Λ). It depends on i and on the sign of D. This result differs from the result obtained for inhomogeneous plane waves propagating in perfectly elastic isotropic media, where the attenuation angle γ always equals 90^0 and is independent of i.

The attenuation angle γ is closely related to the quantity $\mathrm{Im}\sigma$, see the last equation of (7). Actually, γ is less than 90^0 when $\mathrm{Im}\sigma > 0$, equals 90^0 when $\mathrm{Im}\sigma = 0$, and is greater than 90^0 when $\mathrm{Im}\sigma < 0$. Thus, the quantity D_0 discussed sub 3) plays an important role also in the discussion of the attenuation angle γ. If we change the inhomogeneity parameter from $D = 0$ to $D = D_0$, the attenuation angle γ changes from 0^0 to 90^0.

In Fig.2, the propagation angle i equals 45^0. Specific behaviour of individual curves remains qualitatively similar to those displayed in Fig.2 also for other propagation angles i, but may differ in details. Fig.3 shows the same curves for the same model as Fig.2; only the propagation angle i is changed from 45^0 to 135^0. The most distinct differences between Figs.2 and 3 are as follows: a) The maximum values $\mathcal{C}^M$ of the phase velocity are shifted from the region $D < 0$ to the region $D > 0$. b) The minimum values A_{min} of the attenuation curves are shifted from the region $D > 0$ to the region $D < 0$, and the difference between individual curves is greater. c) The quantity Imσ increases with increasing D, and is zero for $D = D_0 < 0$. d) Consequently, $\gamma(-D) > \gamma(D)$ for $D > 0$ in this case. e) For perfectly elastic anisotropic medium, $\gamma = 60.95^0$ for $D > 0$, $\gamma = 119.05^0$ for $D < 0$. Thus, the deviation of γ from 90^0 corresponding to the perfectly elastic isotropic case makes nearly 30^0. Otherwise, all the conclusions made for Fig.2 remain valid.

The attenuation angle γ is closely related to the so-called forbidden directions, see discussion in Section 5.

3.3 SH plane waves in a symmetry plane of anisotropic viscoelastic media: variations with the propagation angle i

Here we discuss the properties of SH plane waves as functions of the propagation angle i, for selected values of inhomogeneity parameter D. We use the polar graphs, with $i = 0^0$ upwards, $i = 90^0$ to the right, see (4). In all cases, the presented polar graphs display the absolute values of the relevant quantities (the signs of these quantities are not distinguished). Instead of the attenuation angle γ, we present $\cos\gamma$. If the quantity $\cos\gamma$ passes through the center of the polar graph, the relevant value of γ passes through 90^0. Moreover, also the quantity Imσ passes through the center of the polar graph in this case.

Fig.4 shows the polar graphs for the same models as those used in Fig.2, for $D = 0.02$. We remind the reader that the black curve corresponds to the model (11), the red and green curves to the twice and four times lower dissipation, and the blue curve to the relevant perfectly elastic anisotropic medium.

The polar graphs of the phase velocity $\mathcal{C}$ and of the attenuation $|\mathbf{A}|$ are quite smooth, and never pass through the center of the graph. The polar graphs for Imσ and $\cos\gamma$ are more complicated. In perfectly elastic media (blue) and in weakly dissipative media (green curves), the curves have four lobes. The polar graphs for $\cos\gamma$ and Imσ are similar in shape in this case. Simple explanation of this similarity follows from the last equation of (7), which yields $\cos\gamma \doteq \epsilon\mathrm{Im}\sigma/|D|$ for $(\mathrm{Im}\sigma)^2 \ll D^2$. For perfectly elastic medium (blue), the shapes of the curves for Imσ and $\cos\gamma$ are practically identical, scaling factor being the value of D, $D = 0.02$. The propagation angles i specifying the boundaries between the lobes correspond to zero values of $\cos\gamma$, i.e., to $\gamma = 90^0$. Consequently, the neighbouring lobes correspond to the attenuation angles $\gamma < 90^0$ and $\gamma > 90^0$.

In Fig.5, the model (11) is considered and the inhomogeneity parameter D is varied, from $D = 0.005$ (black), to 0.02 (red), 0.08 (green) and 0.32 (blue). The red curves in Fig.5 thus correspond to black curves in Fig.4. We can see that the four lobes of Imσ are now generated by increased strength of the inhomogeneity parameter D. Other phenomena are similar to those in Fig.4.

To conclude this section, we can say that the behaviour of the polar graphs for Imσ

and $\cos\gamma$ are often rather complicated. Complexity increases with decreasing dissipation or with increasing $|D|$.

4 Plane waves in general viscoelastic anisotropic media

In the preceding sections we considered the case of SH waves propagating in a symmetry plane of a viscoelastic anisotropic medium, which allows derivation of explicit analytic formulae and their simple analysis. In this section we present and discuss results obtained by numerical solution of Eq.(3). In this way, we can investigate arbitrary isotropic or anisotropic, perfectly elastic or anelastic, homogeneous and inhomogeneous plane waves. We concentrate on inhomogeneous and homogeneous plane waves propagating in a cracked porous/permeable medium of hexagonal symmetry whose moduli were obtained by Jakobsen et al. (2003). To generate the model, the authors used elastic moduli of quartz with pores filled with water and supplemented by a relatively high concentration of nearly fully aligned flat cracks. We choose the model corresponding to the frequency of approximately 35 Hz shown in their Fig.2. For simplicity, we consider unit density. The matrix of complex-valued, density-normalized viscoelastic moduli of hexagonal symmetry with vertical axis of symmetry, measured in GPa then reads:

$$\mathbf{A} = \mathbf{A_1} - \mathrm{i}\mathbf{A_2}, \tag{14}$$

where

$$\mathbf{A_1} = \begin{pmatrix} 46.631 & 5.983 & 4.278 & 0. & 0. & 0. \\ & 46.631 & 4.278 & 0. & 0. & 0. \\ & & 19.931 & 0. & 0. & 0. \\ & & & 13.444 & 0. & 0. \\ & & & & 13.444 & 0. \\ & & & & & 20.324 \end{pmatrix}$$

and

$$\mathbf{A_2} = \begin{pmatrix} 0.033 & 0.022 & 0.156 & 0. & 0. & 0. \\ & 0.033 & 0.156 & 0. & 0. & 0. \\ & & 1.312 & 0. & 0. & 0. \\ & & & 0.055 & 0. & 0. \\ & & & & 0.055 & 0. \\ & & & & & 0.005 \end{pmatrix}.$$

For the above set of moduli, we calculate phase velocities $\mathcal{C}$, attenuation angle γ or its cosine, the quantity $\mathrm{Im}\sigma$, the attenuation $|\mathbf{A}|$ and particle motion diagrams of qP wave and of two qS waves. We first study the listed parameters as functions of the inhomogeneity parameter D, with the propagation angle i fixed, then as functions of propagation angle i with D fixed.

4.1 Plane waves in general anisotropic viscoelastic media: variations with D

In Fig.6, we can see the variation of the phase velocity, of $\mathrm{Im}\sigma$, of the attenuation $|\mathbf{A}|$ and of the attenuation angle γ in the plane of symmetry Σ^S of the model of the viscoelastic anisotropic medium (14). The propagation-attenuation plane $\Sigma^{\|}$ coincides again with the symmetry plane Σ^S. The propagation angle is fixed, $i = 45^0$, and the inhomogeneity parameter D varies from -0.2 to 0.2. The red colour corresponds to the fastest wave. According to its polarization, it is the qP wave. The black colour corresponds to the faster of the qS waves. It has SH-wave polarization. Finally the blue colour is reserved for the slowest wave, which has the qSV-wave polarization. We can see that the phenomena observed in Figs.2 and 3, devoted to SH waves, can be also observed on remaining waves.

1) The **non-symmetricity** with respect to $D = 0$ is most pronounced in the plot of the attenuation angle. But it can be observed in all presented quantities for all waves.

2) Thorough inspection reveals that the maxima of the **phase velocities** of all three waves are shifted slightly towards positive values of D. Thus, the homogeneous waves ($D = 0$) do not propagate with maximum phase velocities as it is the case in isotropic media. They would if we have chosen the propagation angle i along the axis of symmetry or perpendicularly to it.

3) We can see that behaviour of $\mathbf{Im}\sigma$, which controls exponential decay of amplitudes along the direction of propagation $\mathbf{N}$, is very similar to that of SH waves in Fig.2. Variation with D is again nearly linear, thus linearized formulae could be used for its approximation. The slope of the curves differs, being greatest for the fastest wave and smallest for the slowest wave. Each wave has different value of D_0, for which $\mathrm{Im}\sigma = 0$. For $D > D_0$ each wave attains negative values of $\mathrm{Im}\sigma$, which means that the phenomenon of amplitudes of inhomogeneous plane waves growing in the direction of propagation, discussed in Sec.3.2 for SH waves, holds for all three waves propagating in viscoelastic anisotropic media.

4) Although the model used in this study differs considerably from the model (11) used for the SH waves, qualitative and quantitative behaviour of the **attenuation** is very similar. More pronounced differences can be found only for very small values of D. As in the case of SH waves, there is a shift of minima of individual waves from the value $D = 0$ (homogeneous wave) but the shift is very small. The minimum values of the attenuation are nearly zero.

5) The **attenuation angle** γ is zero for $D = 0$ but otherwise behaviour of the curves for individual waves is strongly non-symmetric. The non-symmetricity increases with increase of the phase velocity of the wave. Similar observation holds also for the speed of variation of γ in the vicinity of $D = 0$. As in the case of SH waves, we can see that the boundary attenuation angles γ^* for $D \to -\infty$ and $D \to \infty$ differ. For $D \to -\infty$, γ^* is less than 90^0, for $D \to \infty$, it exceeds 90^0.

Similar phenomena as above could also be observed for other angles of propagation i. Only their intensity would change.

4.2 Plane waves in general anisotropic viscoelastic media: variations with the propagation angle i

Now we study properties of the qP and qS waves as functions of the propagation angle i for several selected values of the inhomogeneity parameter D in the symmetry plane Σ^S of the model of the viscoelastic anisotropic medium (14). Again, the propagation-attenuation plane coincides with the symmetry plane. As before, the red colour indicates the fastest, the black colour intermediate and blue colour the slowest wave. We present polar plots, in which $i = 0^0$ upwards, $i = 90^0$ to the right, see Eq.(4). In all cases absolute values of the studied quantities are shown although some of them like $\cos(\gamma)$ or Imσ may change their sign.

In Fig.7, **phase velocity** polar graphs for four values of the inhomogeneity parameter D, $D = 0$ (homogeneous wave), $D = 0.057$, $D = 0.059$ and $D = 0.2$ are shown. For $D = 0$, the phase velocities are symmetric with respect to the vertical axis. The highest (red) phase-velocity surface is separated from the remaining velocities and corresponds to the qP wave. The higher of the remaining velocities corresponds to the SH wave, see particle motion diagram in Fig.11, the slower to the qSV wave. Both qS-wave phase velocities touch on the vertical axis. For increasing values of D, the qP-wave and qSV-wave phase velocity curves deform ($D = 0.057$) close to the vertical axis and approach each other. The qSV-wave phase velocity curve intersects the SH-wave curve. Therefore, the relevant part of the qSV-wave phase velocity is black in Fig.7. The phase velocities are no more symmetric with respect to the vertical axis. With increasing D the plots of the qP- and qSV-wave velocities get into contact, i.e., for the corresponding propagation angle i (which is non-zero), the qP and qSV waves propagate with the same phase velocity. With further increase of D, the phase velocities decrease (they become zero for $|D| \to \infty$) and all three phase-velocity curves become nearly indistinguishable. Let us emphasize that the individual plots in Fig.7 show phase velocities corresponding to the slowness vector (1) with a selected *constant inhomogeneity parameter* D. Except for $D = 0$ (which corresponds to $\gamma = 0^0$ or 180^0, see Eq.(7)), the plots corresponding to a slowness vector with a *fixed attenuation angle* γ would be different.

In viscoelastic or perfectly elastic *isotropic* media, the relevant curves for phase velocities of both qP and qS waves would be circular.

Fig.8 shows the polar plots of the absolute values of the **quantity Imσ** for four values of D, $D = 0$, $D = 0.01$, $D = 0.059$ and $D = 0.1$. We can see that the plots have quite complicated character, with several lobes. For the case of homogeneous waves ($D = 0$), the plots are symmetric with respect to the vertical and horizontal axes. The qP and SH waves have two lobes extended along the vertical axis. In the horizontal direction, the values of Imσ are effectively zero. The qSV wave (blue) has four lobes. All the values of Imσ for $D = 0$ are positive. With increasing D, the symmetricity of the plots with respect to the vertical disappears and the plots further complicate. For $D = 0.01$, each of the three waves has four lobes. The lobes of the qSV wave are related again to positive values of Imσ. The new (smaller) lobes of the qP and SH waves, however, are related to negative values. This means that in the corresponding directions, amplitudes of the qP and SH waves increase in the direction of propagation. The plot for $D = 0.059$ corresponds to the value of D for which the qP- and qSV-wave phase velocity curves get into the contact, see

Fig.7. We can see that the number of lobes of the qS waves again increased. The number of lobes of qP and SH waves is four as for $D = 0.01$. The number of lobes of the qSV wave increased to eight! The increased number of lobes is related to the intersection of the two qS-wave phase velocity sheets. The number of lobes is eight already for $D = 0.057$. Also note the increase of the absolute value of Imσ. A closer inspection reveals that some of the lobes change abruptly colour from blue to black and vice versa. This is a consequence of the fact that the colours do not correspond to wave modes defined by their polarization. When we increase D to $D = 0.1$, the number of lobes of each wave is again four. We can, however, observe abrupt changes of all three colours. This is because the phase velocities of all the three waves are interconnected, see Fig.7. Some lobes of each wave are related to negative values.

In a viscoelastic *isotropic* medium, the curve of Imσ would be circular for each wave. In an elastic isotropic medium, it would reduce to a point.

In Fig.9, behaviour of the **attenuation** $|\mathbf{A}|$ is illustrated in plots corresponding to $D = 0$, $D = 0.001$, $D = 0.005$ and $D = 0.01$. For small values of D, behaviour of the attenuation is very similar to that of Imσ. This is obvious from Eqs.(7). For $D = 0$, $|\mathbf{A}| = |\mathrm{Im}\sigma|$. For small values of D, attenuation is more anisotropic than phase velocity. This is in agreement with observations made by Hosten et al. (1987). Hosten et al. (1987) also observed directions in which, in contrast to isotropic media, qP-wave attenuation was larger than qS-wave attenuation. In our case, such a direction is the direction along the axis of symmetry. In the direction perpendicular to the axis of symmetry, the attenuation is small and nearly equal for all waves. Anisotropy of the attenuation of all three waves decreases considerably with increasing D while $|\mathbf{A}|$ itself increases. Attenuation of the SH wave (black) has, except for the case of a homogeneous wave, nearly circular character for any non-zero value of D. In the horizontal direction, the attenuation of all three waves is equal for non-zero D.

For viscoelastic isotropic media, the curves in Fig.9 would be circular. For perfectly elastic isotropic media, the radius of the circles would be $|D|$.

Very interesting is behaviour of the **attenuation angle** γ, specifically of absolute value of $\cos\gamma$, which is shown in Fig.10. For $D = 0$, cosines of the attenuation angles γ of qP and qS waves are unit, i.e., $\gamma = 0$, which indicates homogeneous waves. For D=0.0001, cosine corresponding to the qSV wave remains nearly unit. The diagram is only slightly reduced in the horizontal direction. Cosines of the qP and SH waves are unit only in a vicinity of the vertical direction. They are both minimum in the horizontal direction. For $D = 0.001$, the cosine of the qP wave has four lobes. Two big lobes are along vertical axis and correspond to positive values of $\cos\gamma$, i.e. to values of γ less than 90^o. Two very small hardly visible lobes correspond to negative values of $\cos\gamma$, i.e. to values of γ greater than 90^o. The qSV wave has also four-lobe character with γ always less than 90^0. The SH-wave curves consist of two lobes only with nearly-vertical orientation and significantly reduced size, which means that the attenuation angle γ is for all directions of propagation considerably different from zero. This is not true for qP and qSV waves, for which there are directions , in which the angle γ is zero or close to zero. This situation changes considerably when D is further increased. For $D = 0.01$, the angles γ of all waves differ considerably from zero. The curves of $\cos\gamma$ of all waves have now four-lobed character. The smaller lobes of qP and SH waves have negative values, all lobes of the qSV wave have positive values. For $D \geq 1$, the plots of cosines of the attenuation angle become insensitive to the variation of D. This means that the plot for $D = 1$ can be taken as an approximation of the plot of $\cos\gamma^*$, i.e. of the cosine of the boundary attenuation angle. The values of γ greater than γ^* correspond to the forbidden directions discussed in Sec.5. Note that as in Figs.2 and 3, γ^* is generally different from 90^0. Since values of $\cos\gamma$ are negative in the bottom left – upper right direction, the angles γ^* are larger than 90^0 in these directions. For the bottom right – upper left direction, the angles γ^* are less than 90^0.

Let us note that in viscoelastic *isotropic* media, all curves for qP and qS waves would be circular and would always correspond to positive values of $\cos\gamma$, indicating that the attenuation angle is directionally independent and $0^0 < \gamma < 90^0$. The angle γ would become 90^0 for perfectly elastic isotropic medium.

Behaviour of **polarization** of all the three discussed waves is shown in Fig.11. The polarization vectors are calculated from Eq.(2). The vectors $\mathbf{U}$ are normalized so that $U_i U_i^* = 1$. Particle motion diagrams show several interesting phenomena. We can see that even for $D = 0$, i.e. for homogeneous waves, the particle motion of qP and qSV waves is elliptical in all directions except some specific directions. For the directions along and perpendicular to the axis of symmetry of the medium (14), the polarization of homogeneous waves is linear. In this respect, it is interesting to note that for $D > 0$, i.e., for inhomogeneous waves, the strongest elliptical polarization of qP and qSV waves can be observed along the vertical. Since we study plane waves in the symmetry plane of the medium (14), SH-wave polarization is always linear, no matter which value of D is considered, and perpendicular to the plane of the plots. We can also see that with increasing D, it becomes more and more difficult (and for D greater than shown in Fig.11 even impossible) to distinguish qP and qSV waves according to their polarization. Another interesting phenomenon are black ellipses along the vertical for $D = 0.05$ and 0.1. They indicate that the qSV wave is no more the slowest wave in this direction. The slowest is now the SH wave, see Fig.7. Finally we can see that increase of value of D destroys the symmetry of the plots with respect to the vertical.

Sofar we studied behaviour of various characteristics of plane waves propagating so that the propagation-attenuation plane $\Sigma^{\|}$ coincided with the symmetry plane Σ^S of the viscoelastic anisotropic media. There is no problem to make similar studies in planes $\Sigma^{\|}$, different from the symmetry planes. We would find that most of the above observed phenomena are observable in these cases as well, the plots being only slightly more complicated. As an example, we show behaviour of polarization in the vertical plane $\Sigma^{\|}$ through the model (14) rotated first by 45^0 around the x_3 axis and then again by 45^0 around the new x_2 axis. Because $\Sigma^{\|}$ does no more coincide with the symmetry plane, we can observe polarization of all three waves in Fig.12. It is interesting to note that the elliptical polarization is reduced with respect to Fig.11, especially for $D = 0$. For $D \geq 0.05$, it becomes difficult to distinguish the two qS waves, at least in the presented plots.

5 Explanation of forbidden directions in directional specification

The mixed specification offers simple explanation of the phenomenon of *forbidden directions*, first discovered in pioneering works of Krebes and Le (1994), and Carcione and Cavallini (1995). These authors used the directional specification of the slowness vector, and specified the slowness vector by the propagation angle i and the attenuation angle γ. For γ fixed, they obtained negative values of $\mathcal{C}^2$ for certain propagation angles i. This result was interpreted in such a way that these propagation directions i are forbidden for inhomogeneous plane waves with γ given or larger. The above result indicates that the specification of the slowness vector by fixed attenuation angle γ is connected with certain problems. Indeed, use of the mixed specification by Červený and Pšenčík (2004) and in this paper showed that γ must always be less than the boundary attenuation angle γ^*, which means that γ cannot be chosen arbitrarily. The determination of γ^* within the directional specification of the slowness vector is, however, very difficult if not impossible. For this reason, it is more reasonable to use the inhomogeneity parameter D, which is subjected to no restrictions for the specification of the slowness vector.

For simplicity, let us illustrate the problem of forbidden directions on the case of inhomogeneous SH plane waves propagating in the model (11). The model resembles closely the model used by Carcione and Cavallini (1995) to study forbidden directions. Carcione and Cavallini (1995) showed that, for fixed $\gamma > 64^0$, two regions of forbidden directions are formed close to propagation angles $i = 135^0$ and 315^0. Let us have a look at this problem in the i, γ and i, D domains.

The upper plot of Fig.13 shows squares of the phase velocities $\mathcal{C}^2$ for four fixed values of γ, the middle and bottom plots show the phase velocities $\mathcal{C}$ and the attenuation angle γ for four fixed values of D, all as functions of the propagation angle i. The curves of $\mathcal{C}^2$ in the upper plot are parameterized by the following values of the attenuation angle γ: $\gamma = 25^0$ (black), $\gamma = 58^0$ (red), $\gamma = 60^0$ (green) and $\gamma = 62^0$ (blue). This plot corresponds qualitatively to Fig.4.6 of Carcione (2001). We can see that for $\gamma = 25^0$ and 58^0, the curves attain positive values of $\mathcal{C}^2$ for any propagation angle i. For $\gamma = 60^0$ and 62^0, however, we can observe that $\mathcal{C}^2$ attains negative values for some angles i. These represent the forbidden directions.

In the middle plot, the phase velocities $\mathcal{C}$ are parameterized by the inhomogeneity parameters D: $D = 10$ (black), $D = 1$ (red), $D = 0.03$ (green) and $D = 0.01$ (blue). The green and blue curves practically coincide. The bottom plot shows behaviour of the attenuation angles γ corresponding to the mentioned fixed values of D. For D greater than, say, 1, the values of γ practically do not change with D increasing. Consequently, the curves of γ for $D = 1$ and $D = 10$ practically coincide, and can be considered as the boundary attenuation angle γ^*. All curves in the middle and bottom plots are smooth and simple; they do not display any negative values of $\mathcal{C}$.

Let us have a closer look at the boundary attenuation angle γ^*, represented by the uppermost curve in the bottom plot of Fig.13. We can see that the boundary attenuation angle γ^* depends strongly on the propagation angle i; it has two minima $\gamma^*_{min} = 60.5^0$ at $i = 135^0$ and $i = 315^0$, and two maxima $\gamma^*_{max} = 119.4^0$ at $i = 15^0$ and $i = 195^0$.

For a given propagation angle i, the inhomogeneous plane waves with the attenuation angle γ greater than the boundary attenuation angle γ^* **do not exist**. Thus, for any fixed $\gamma < \gamma^*_{min}$, the inhomogeneous plane waves exist for any propagation angle i. For $\gamma^*_{min} < \gamma < \gamma^*_{max}$, two forbidden regions are developed in the i, γ domain. In our case, the first is concentrated around $i = 135^0$, and the second around 315^0. Finally, for $\gamma > \gamma^*_{max}$, inhomogeneous plane waves do not exist for any propagation angle i.

Let us consider, as an example, a fixed attenuation angle $\gamma = 62^0$, see the horizontal black line in the bottom plot of Fig.13. Then the boundaries of the forbidden regions (intersections of the uppermost curve corresponding to γ^* with the horizontal black line) in the bottom plot correspond exactly to the intersections of the blue curve ($\gamma = 62^0$) with zero in the upper plot.

6 Conclusion

The mixed specification, based on the use of unit vectors **n** and **m**, and the inhomogeneity parameter D, can be used to study propagation of homogeneous or inhomogeneous waves propagating in elastic or viscoelastic, isotropic or anisotropic media. Problems with non-physical results related to forbidden directions, which exist in the directional specification, do not exist in the mixed specification. On the contrary, the mixed specification offers a simple way of calculation of the boundary attenuation angles specifying which attenuation angles are allowed and which not. In case of SH plane waves, the mixed specification yields explicit analytic expressions, which can be easily analyzed.

The results obtained with the mixed specification show several phenomena unknown from studies of wave propagation in perfectly elastic isotropic or anisotropic and viscoelastic isotropic media. Most of them have been predicted by analysis of simple analytic formulae describing plane wave propagation in a symmetry plane of a viscoelastic anisotropic medium in Červený and Pšenčík (2004). For example, it was shown that, in contrast to the wave propagation in viscoelastic isotropic media, the maximum phase velocity in a given direction might not be associated with the homogeneous wave. Similarly, the minimum attenuation might not be associated with the relevant homogeneous wave. The amplitudes of inhomogeneous waves may increase exponentially in the direction of propagation. Except for some special directions, polarization of all waves is, in general, elliptical.

As in Červený and Pšenčík (2004), we considered plane waves throughout the paper. We consider such study as a necessary step before solving problems of propagation of general waves in general types of media.

Acknowledgements

The authors are greatly indebted to Luděk Klimeš for helpful suggestions and valuable discussions. Thanks to Morten Jakobsen for providing the data for numerical tests. The research has been supported by the Consortium Project "Seismic Waves in Complex 3-D Structures", by the Research Project 205/04/1104 of the Grant Agency of the Czech Republic, by the Research Project A3012309 of the Grant Agency of the Academy of Sciences of the Czech Republic, by the Ministry of Education of the Czech Republic under Research Project MSM113200004, and by the Academy of Sciences within research projects Z3012916 and K3012103. Part of this work has been done during the IP's stay at the University of Hamburg sponsored by the DFG project TSE 17/5/02 within Ga 350/10-1.

References

Aki, K., and Richards, P., 1980. *Quantitative seismology. Theory and methods.* Freeman, San Francisco.

Carcione, J.M., 2001. *Wave fields in real media: Wave propagation in anisotropic, anelastic and porous media.* Pergamon, Amsterdam.

Carcione, J.M., and Cavallini, F., 1995. Forbidden directions for inhomogeneous pure shear waves in dissipative anisotropic media. *Geophysics*, **60**, 522–530.

Červený, V., 2004. Inhomogeneous harmonic plane waves in viscoelastic anisotropic media. *Studia Geophys. Geod.*, **48**, 167–186.

Červený, V., and Pšenčík, I., 2004. Slowness vectors in viscoelastic anisotropic media. Part1: Theory. In: *Seismic Waves in Complex 3-D Structures, Report 14*, pp.123–147. Charles University, Faculty of Mathematics and Physics, Dept. of Geophysics, Praha.

Fedorov, F.I., 1968. *Theory of elastic waves in crystals.* Plenum, New York.

Hosten, B., Deschamps, M., and Tittmann, B.R., 1987. Inhomogeneous wave generation and propagation in lossy anisotropic solids. Applications to the characterization of viscoelastic composite materials. *J. acoust. Soc. Am.*, **82**, 1763–1770.

Jakobsen,M., Johansen,T.A., and McCann,C., 2003. The acoustic signature of fluid flow in complex porous media. *J.Appl.Geophys.* **54**, 219–246.

Krebes, E.S., and Le, L.H.T., 1994. Inhomogeneous plane waves and cylindrical waves in anisotropic anelastic media. *J. Geophys. Res.*, **99**, No. B12, 23899–23919.

Press, W.H., Flannery, B.P., Teukolsky, S.A. and Vetterling, W.T., 1986. *Numerical recipes.* Cambridge University Press, Cambridge.

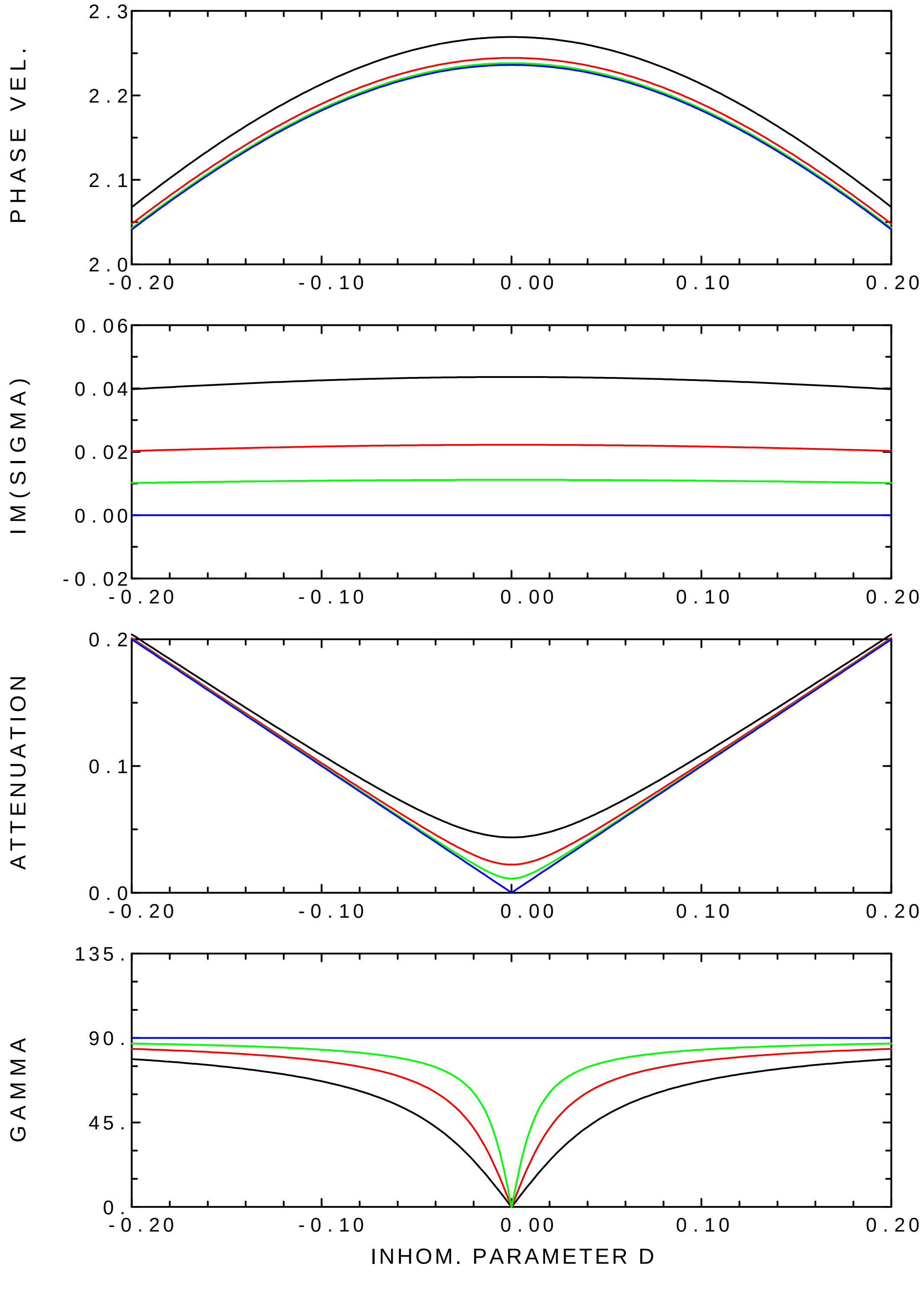

Fig.1: Variations with D of the phase velocity $\mathcal{C}, \mathrm{Im}\sigma$, the attenuation $|\mathbf{A}|$ and the attenuation angle γ of SH plane waves in a viscoelastic isotropic model (13). Colours correspond to varying values of ν in (13): $\nu = 1$ (black), $\nu = 0.5$ (red), $\nu = 0.25$ (green), and $\nu = 0$ (blue; a perfectly elastic isotropic medium).

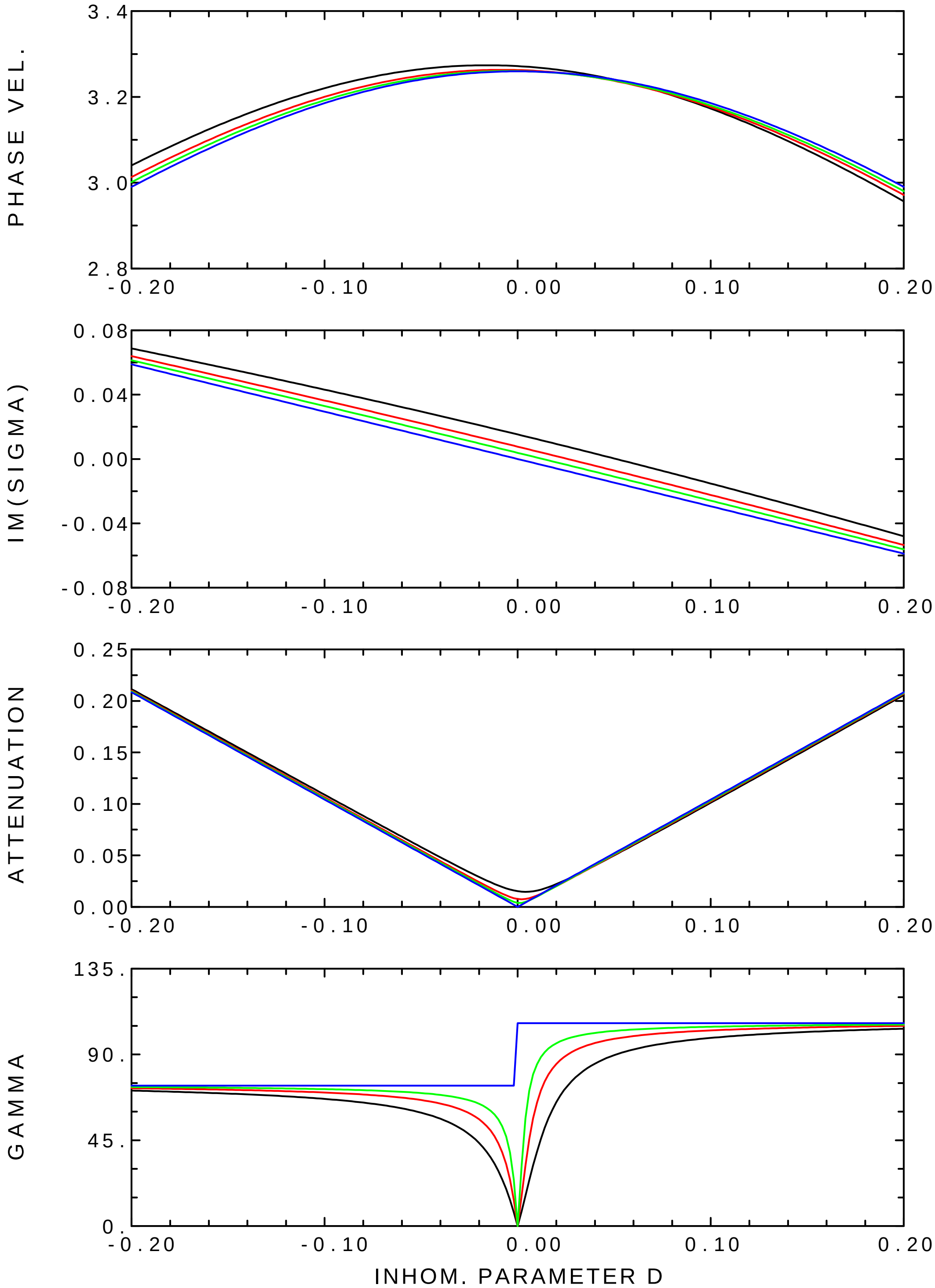

Fig.2: Variations with D of the phase velocity $\mathcal{C}, \mathrm{Im}\sigma$, the attenuation $|\mathbf{A}|$ and the attenuation angle γ of SH plane waves in the medium (11) (black), the medium (11) with the twice and four times smaller imaginary parts (red and green, respectively), and to the medium (11) with zero imaginary parts of viscoelastic moduli (blue; perfectly elastic medium). The propagation angle $i = 45^0$.

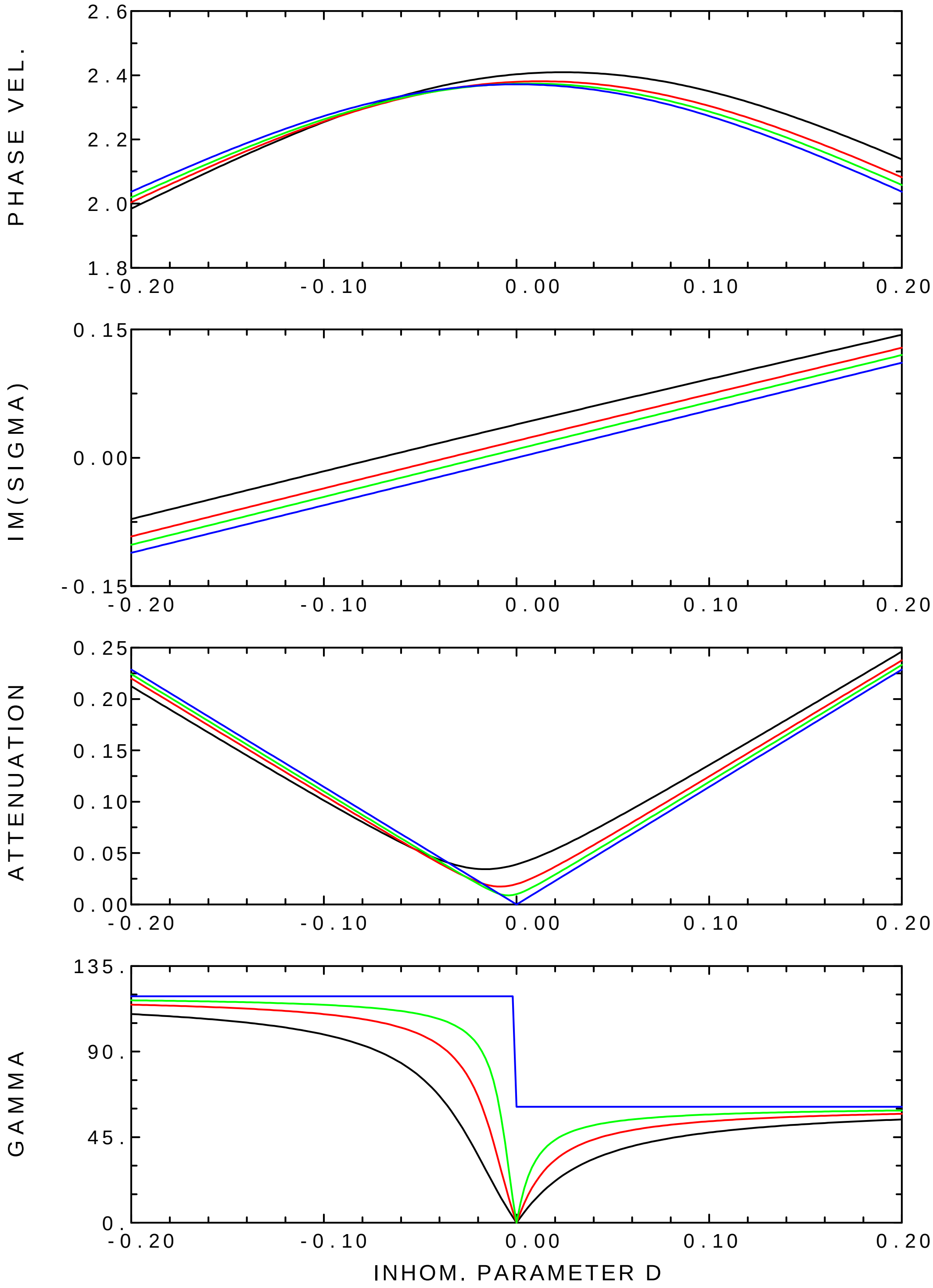

Fig.3: The same as in Fig. 2 but for the propagation angle $i = 135^0$.

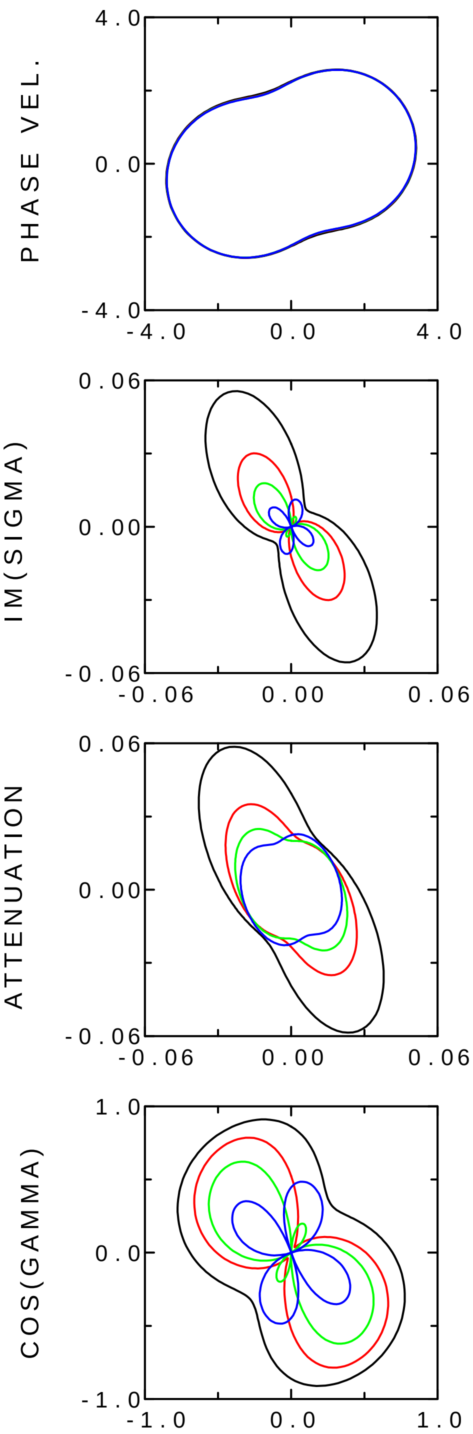

Fig.4: The same as in Fig. 2 but in polar diagrams for the inhomogeneity parameter $D = 0.02$.

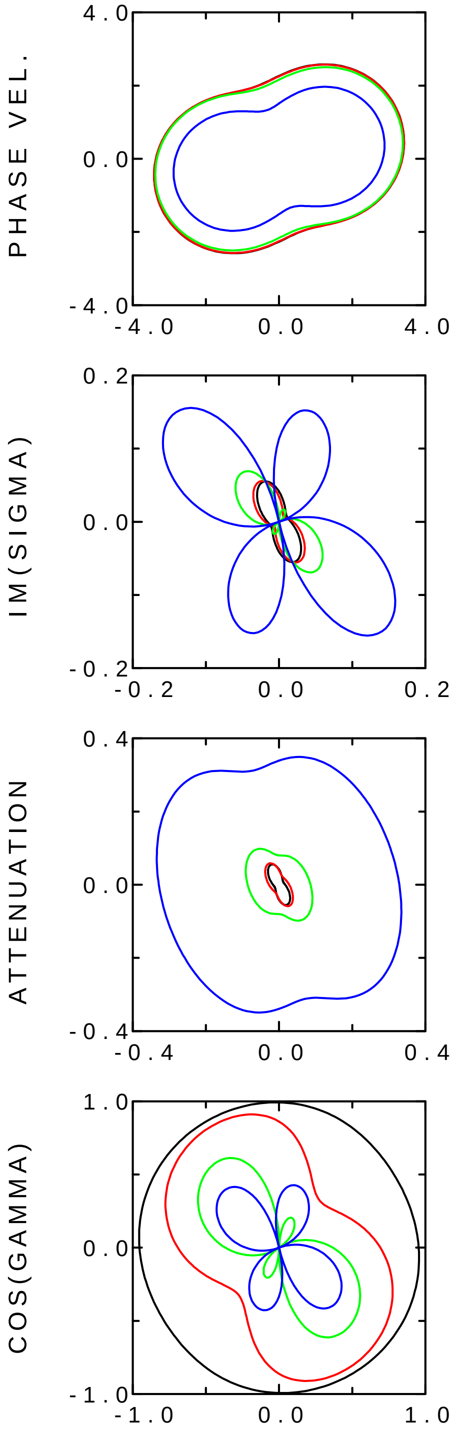

Fig.5: The same as in Fig. 4 but for the model (10). Varying inhomogeneity parameters D: $D = 0.005$ - black, $D = 0.02$ - red, $D = 0.08$ - green, and $D = 0.32$ - blue.

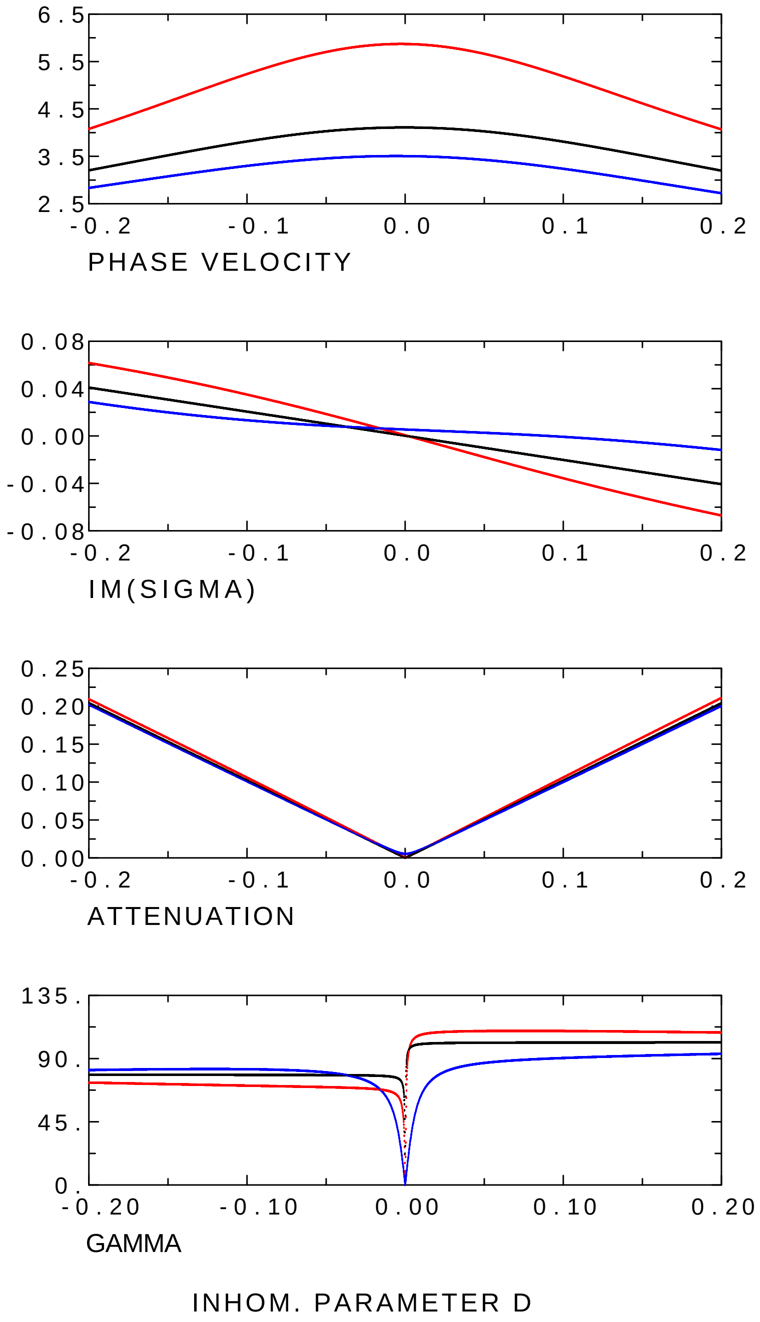

Fig.6: Variations with D of the phase velocity $\mathcal{C}, \mathrm{Im}\sigma$, the attenuation $|\mathbf{A}|$ and the attenuation angle γ of plane waves in a plane of symmetry of the medium (14). Red: the fastest wave (qP wave), black: intermediate wave (SH wave), blue: the slowest wave (qSV wave). The propagation angle $i = 45^0$.

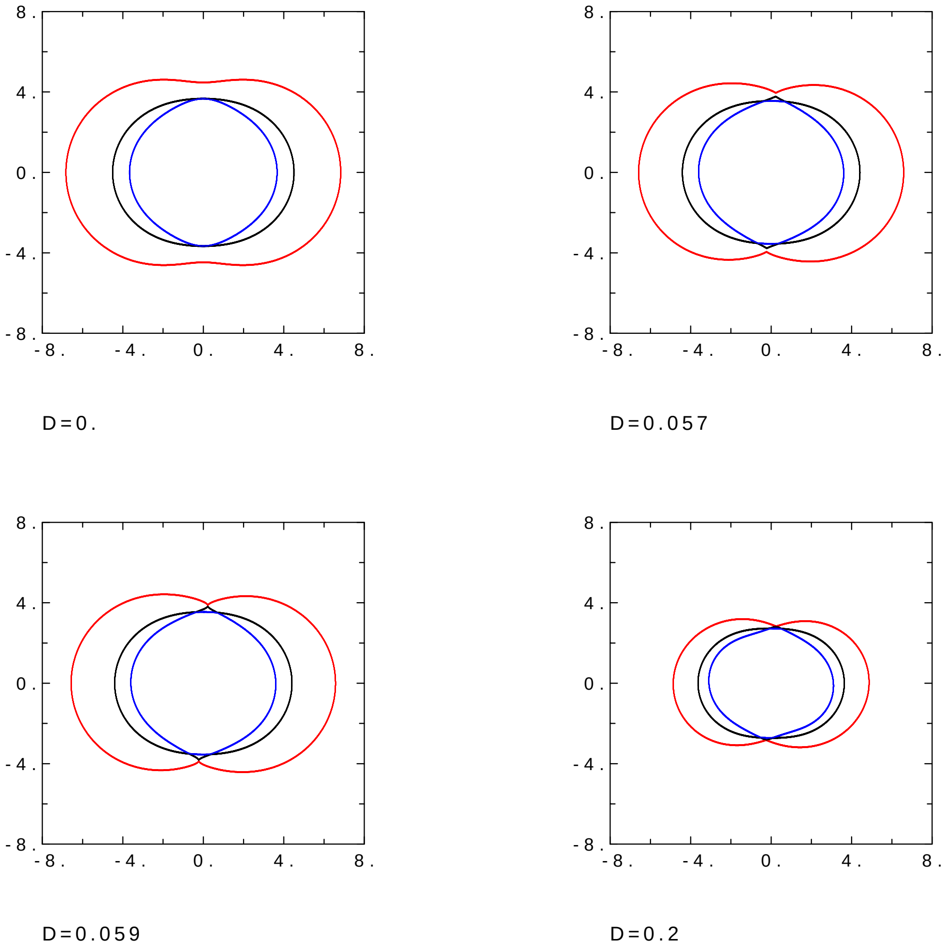

Fig.7: Polar diagrams of the phase velocity $\mathcal{C}$ in a plane of symmetry of the medium (14) for $D = 0$ (homogeneous wave), 0.057, 0.059 and 0.2. Red: the fastest wave (qP wave), black: intermediate wave, blue: the slowest wave. Note that qSV wave is slowest in most directions but intermediate in the vertical direction for $D \geq 0.057$.

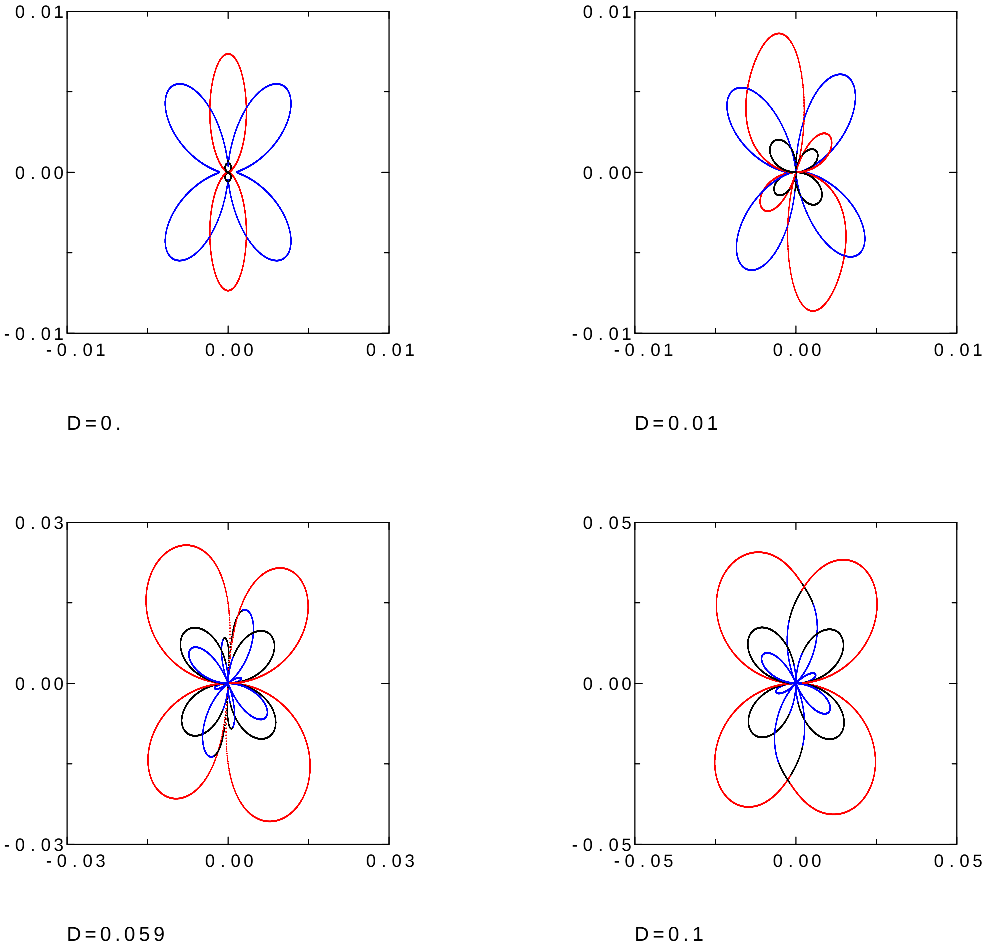

Fig.8: Polar diagrams of $|\mathrm{Im}\sigma|$ in a plane of symmetry of the medium (14) for $D = 0$ (homogeneous wave), 0.01, 0.059 and 0.1. The colours as in Fig.7.

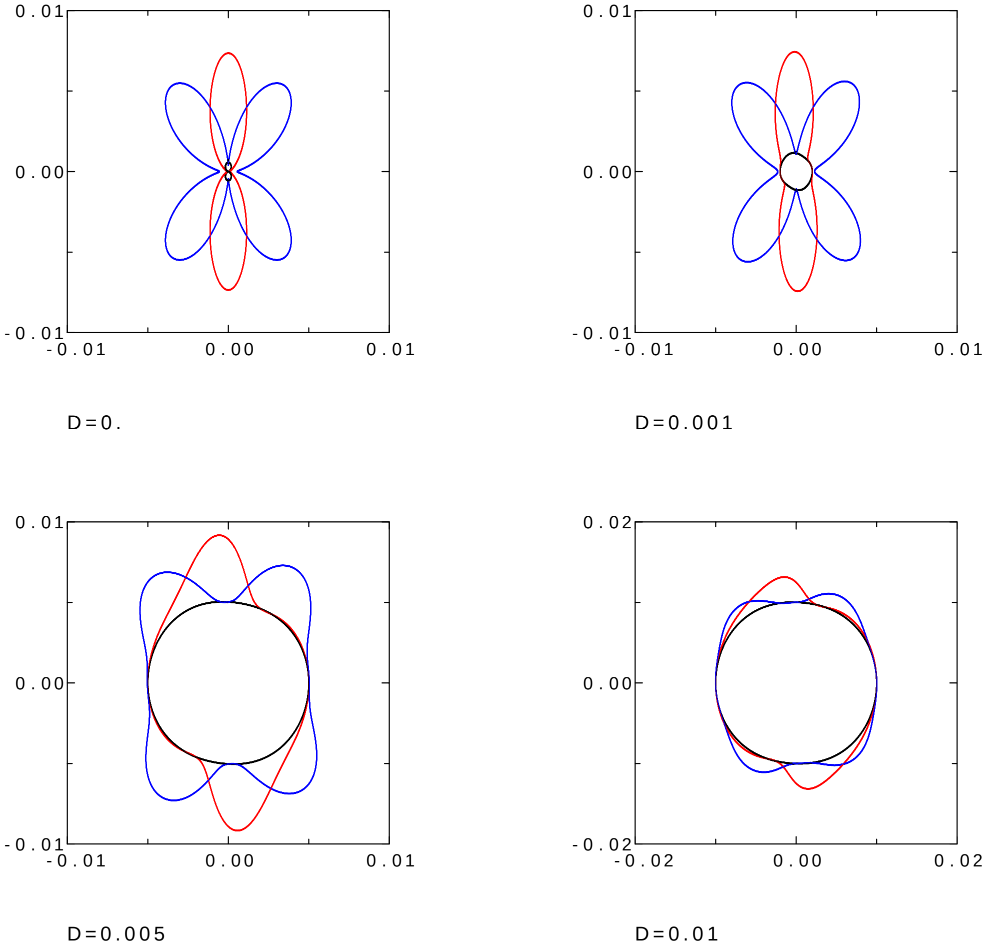

Fig.9: Polar diagrams of the attenuation $|\mathbf{A}|$ in a plane of symmetry of the medium (14) for $D = 0$ (homogeneous wave), 0.001, 0.005 and 0.01. The colours as in Fig.7.

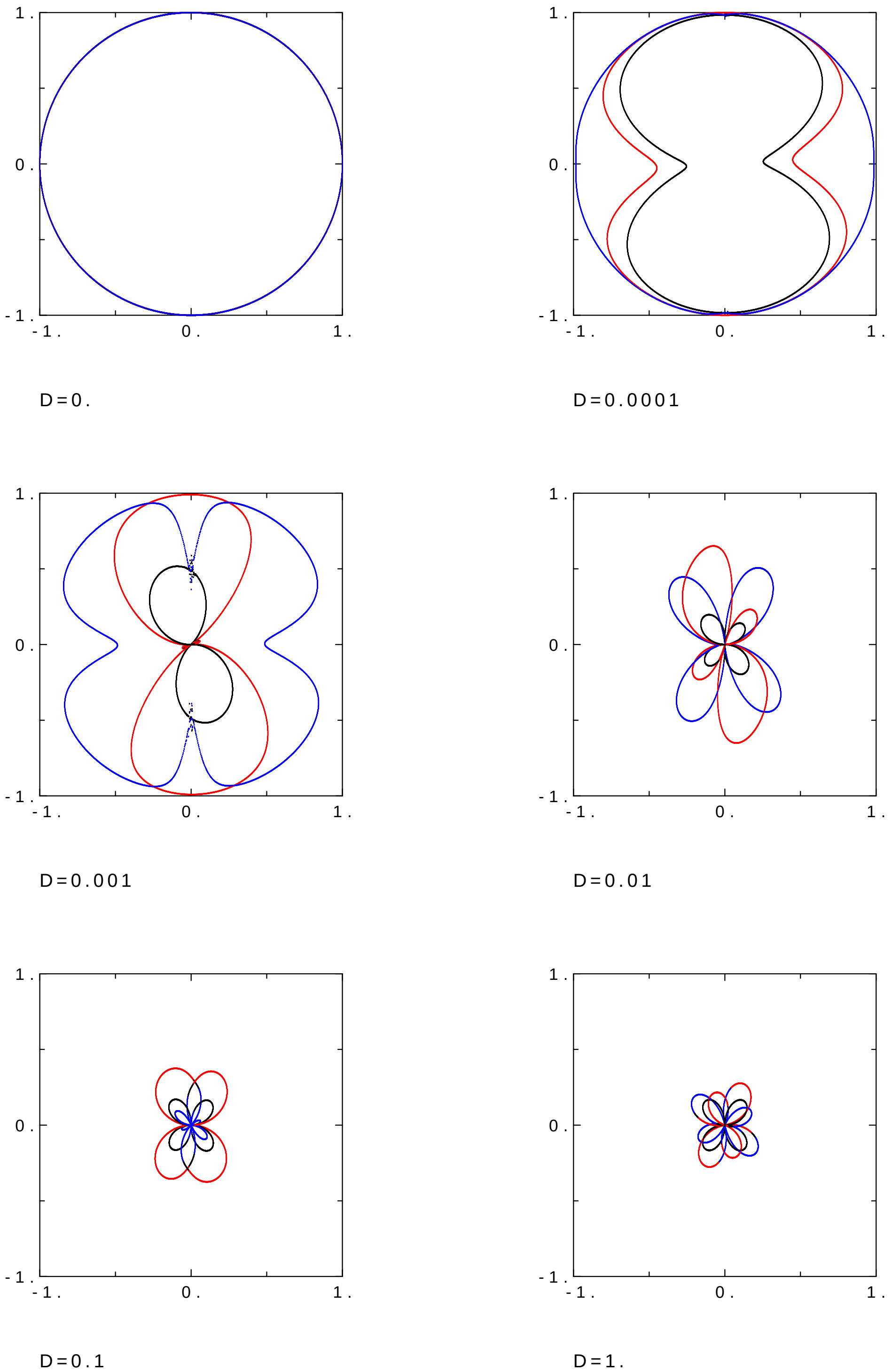

Fig.10: Polar diagrams of $|\cos\gamma|$ in a plane of symmetry of the medium (14) for $D = 0$ (homogeneous wave), 0.0001, 0.001, 0.01, 0.1 and 1. The colours as in Fig.7.

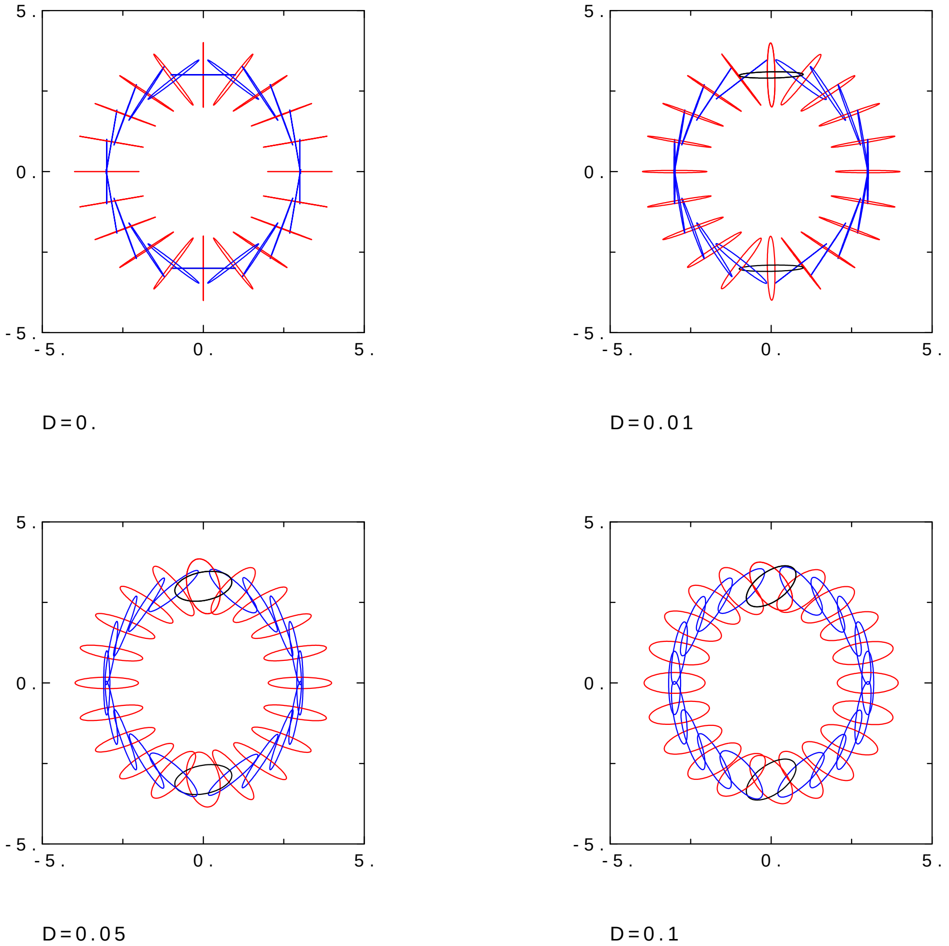

Fig.11: Polar diagrams of the polarization in a plane of symmetry of the medium (14) for $D = 0$ (homogeneous wave), 0.01, 0.05 and 0.1. The colours as in Fig.7. SH-wave polarization is perpendicular to the plots.

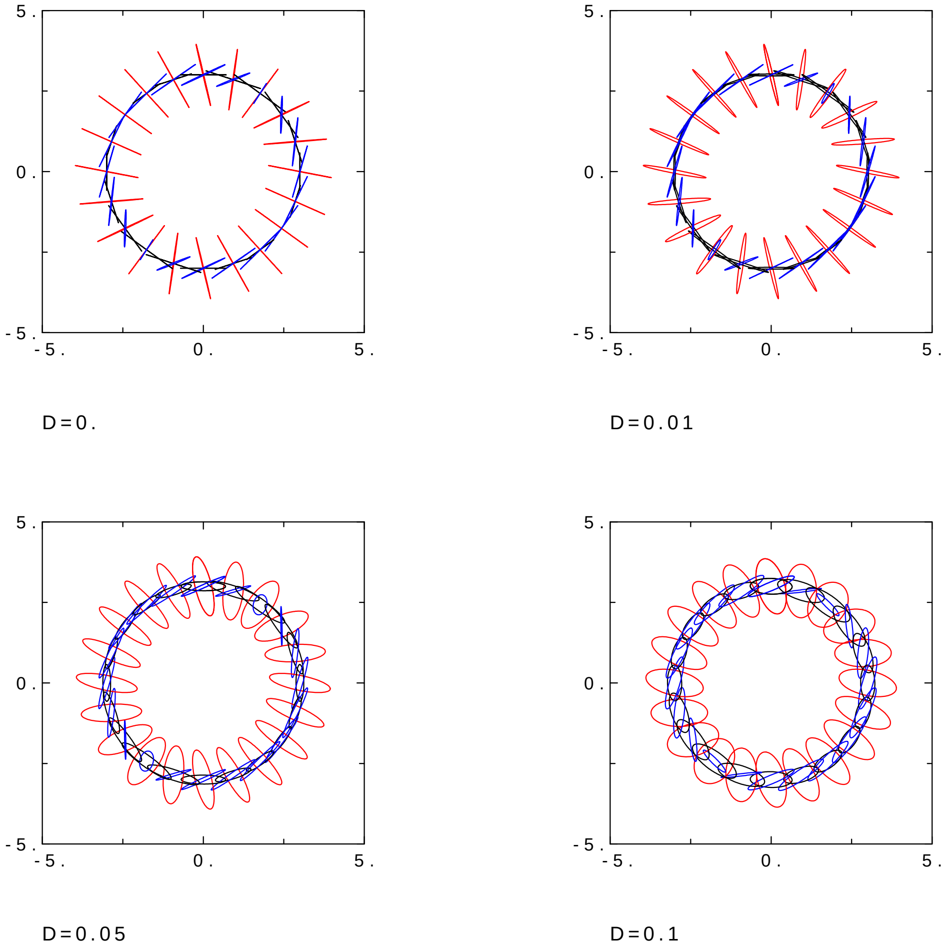

Fig.12: Polar diagrams of the polarization in a rotated model of the medium (14) for $D = 0$ (homogeneous wave), 0.01, 0.05, and 0.1. The colours as in Fig.7.

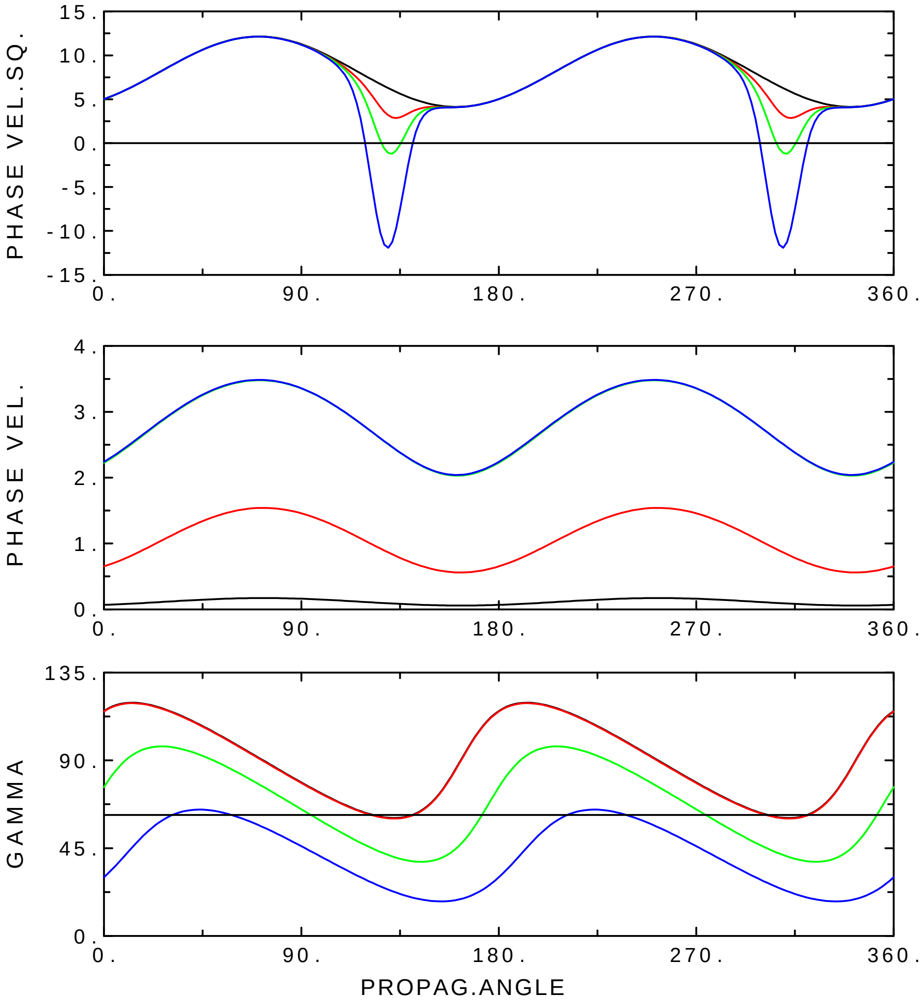

Fig.13: Explanation of the forbidden directions. Inhomogeneous SH plane waves in a plane of symmetry of the anisotropic medium (11). Dependence of $\mathcal{C}^2$, $\mathcal{C}$ and γ on the propagation angle i. The upper plot of $\mathcal{C}^2$ parameterized by γ: $\gamma = 25^0$ (black), $\gamma = 58^0$ (red), $\gamma = 60^0$ (green) and $\gamma = 62^0$ (blue). Note that green and blue curves intersect zero, defining thus forbidden directions. The middle and bottom plots of $\mathcal{C}$ and γ parameterized by D: $D = 10$ (black), $D = 1$ (red), $D = 0.03$ (green), and $D = 0.01$ (blue). For $D \geq 1$, the curves for attenuation angle γ yield the boundary attenuation angle γ^* (uppermost curve in the bottom plot). For $\gamma = 62^0$ (black line in the bottom plot), inhomogeneous plane waves cannot exist for i close to 130^0 and 310^0, where $\gamma > \gamma^*$, i.e., the horizontal line intersects the uppermost curve. For more details see text.